Annals of Glaciology 16 1992

The movement mechanisms of Ürümqi Glacier No. 1, Tien Shan mountains, China

HUANG MAOHUAN
Lanzhou Institute of Glaciology and Geocryology, Academia Sinica, Lanzhou 730000, China

ABSTRACT. Beneath Ürümqi Glacier No. 1, there is an ice-laden till layer which is more than 10 m thick near the terminus. The 0°C isotherm is generally at some depth below the glacier sole and lies within the bedrock below the ice-laden till layer near the terminus. Thus the glacier is entirely cold and impermeable, except for a thin snow–firn layer at its surface and some crevassed areas. Meltwater drains off mainly by surface channels, assisted by subglacial conduits. Four flow mechanisms have been identified in the glacier. They are ice deformation, bed deformation, shear faulting, and sliding over the bed. At the terminus and along the margins, bed deformation can provide a significant contribution to the overall surface motion. Bed deformation consists of creep and discontinuous slip. However, creep experiments on samples taken from the ice-laden till layer provide no positive indication that this layer deforms more easily than clean ice. Discontinuous slip thus may provide the major contribution to bed deformation.

1. INTRODUCTION

Ürümqi Glacier No. 1, Tien Shan mountains, (herein referred to simply as Glacier No. 1) is the principal focus of research at the Tien Shan Glaciological Station, Chinese Academy of Sciences, and the glacier that has been the most intensively studied in China. It is a small cirque-valley glacier consisting of two tributaries, covering an area of 1.865 km^2 from its head at 4479 m a.s.l. to its terminus at 3734 m a.s.l. (Fig. 1). The equilibrium line was at an average elevation of 3976 m during the period 1979 to 1989. The glacier is presently retreating and thinning.

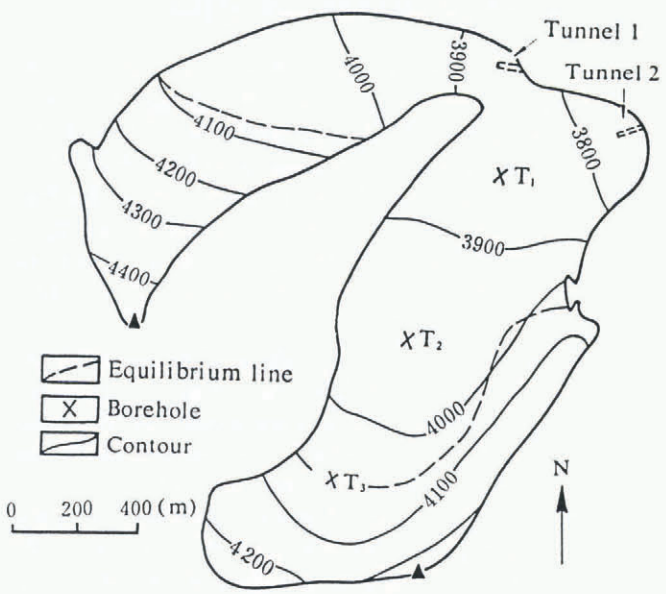

Fig. 1. Map showing the locations of tunnels 1 and 2 and of the three deep boreholes for temperature measurement (T_1, T_2 and T_3).

The ice thickness of both tributaries of Glacier No. 1 was measured by means of radar sounding in August 1981 (Zhang and others, 1985). The maximum thickness is 137 m in the east tributary and 139 m in the west tributary. The maximum thickness appears in the middle of the ablation area of the east tributary and near the equilibrium line of the west tributary.

To determine the englacial thermal regime of Glacier No. 1, temperature measurements were made in deep holes in the east tributary in 1986 (Cai and others, 1988; Cai, 1989). Three holes were bored with a hot-water drill. These holes are located at T_1 (3854 m altitude) and T_2 (3928 m) in the lower and middle parts of the ablation area respectively, and at T_3 (4033 m) near the equilibrium line (Fig. 1). The hole depths are 86, 102 and 106 m, respectively. The ice thickness determined by previous radar sounding was 96, 138 and 106 m for the three locations, respectively.

Studies of movement mechanisms consist of measurements of surface velocity, of deformation and displacement in tunnels 1 and 2 (Fig. 1), and of creep experiments on glacial ice. Echelmeyer and Wang (1987), Huang and Wang (1987), Huang and others (1989) and Huang and others (1990) have presented previous studies.

So far, four movement mechanisms have been identified in Glacier No. 1. They are ice deformation, bed deformation, shear faulting, and sliding over the bed. Bed deformation is the focus of this paper.

https://doi.org/10.3189/1992AoG16-1-39-44 Published online by Cambridge University Press

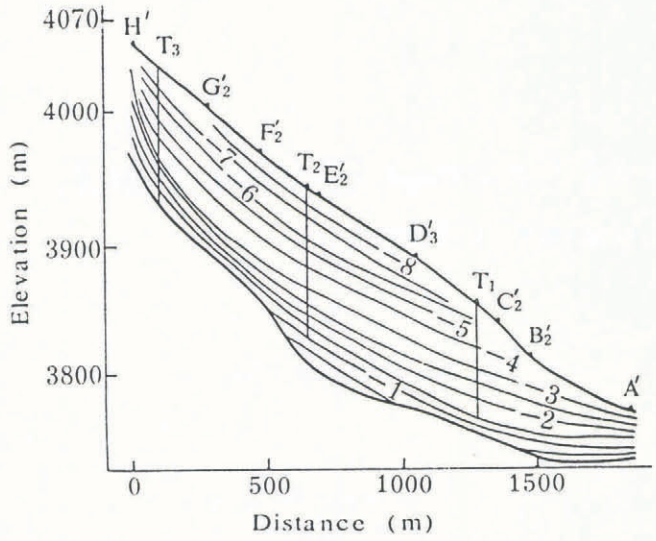

Fig. 2. Modelled two-dimensional temperature profile along the main flowline of the east tributary of Glacier No. 1 (after Cai, 1989).

2. TEMPERATURE REGIME

Huang (1990) has described the temperature regime of Glacier No. 1 as being typical of glaciers of the sub-polar type in China. In the infiltration zone there is a warm firn area which is at the melting point during the summer, as it is, for example, on other sub-polar glaciers such as Storglaciären, Sweden (Hooke and others, 1983). As for the ablation area, Figure 2 shows the two-dimensional temperature profile along the main flowline of the east tributary, based on numerical calculations using a model that includes both diffusion and advection in both horizontal and vertical directions as well as the geothermal flux (Cai, 1989). The model is verified by the measurements in the deep holes. The maximum difference between the model and the measurements is ±0.4°C. In this profile a low temperature regime is present in the top of the upper half of the ablation area, and two warm regions, where the temperature is more than –0.5°C, occur at the base, one in the middle of the ablation area and the other near the terminus. This implies that temperate ice, above –0.5°C, is present in the middle of the ablation area, beneath the thickest part of the glacier and also near the terminus.

Tunnel 2 was excavated in the autumn of 1988. The ice temperature was measured while the tunnel was being extended in order to minimize the error due to disturbance of the temperature field caused by the excavation (Huang, 1990, fig. 6). The temperature in this tunnel was found to be –0.36°C near the back wall, decreasing to –0.8°C near the entrance. According to Huang and others (1990), the temperature gradient at the bottom of the glacier is approximately 0.028 K m^{-1}. Thus it is estimated that the 0°C isotherm lies at a depth of at least 10 m in the bed.

3. WATER FLOW

On the glacier surface, water is confined to a network of streams. At times, water is ponded in a surface lake at the junction of the two branches of the glacier. Some crevasses develop in the west tributary, and these admit water, resulting in an increase in ice temperature. Finally, water is discharged in several surface and ice-marginal channels. In places, a marginal channel cuts into the ice and an englacial conduit is formed. Such a conduit emerges near the entrance of tunnel 2. The temperatures measured in tunnel 2 make it clear that around the conduit the ice is sub-freezing.

To investigate the hydraulic conditions of the glacier, salt tracer experiments were conducted in August 1989 (Kang, 1991). Six injection points were located in the ablation area and one in the accumulation area, immediately above the equilibrium line. There was a single peak in all the concentration-time curves. It took only 1 to 2 h for the meltwater to run to the glacial gauging station, 315 m from the terminus, during the late-season period of maximum development of the glacial drainage system. These observations suggest that the englacial and subglacial conduits are not braided. Storage of meltwater in the glacier is insignificant.

Several surveys between 1 September 1984 and 23 August 1985 (You, 1987) indicate that summer velocities are about 20% greater than winter ones in the bend section of the west tributary, where many crevasses form. However, winter velocities were slightly greater than summer ones in the upper half of the east tributary. There was no significant seasonal variation in other sections of the glacier (Chen and Sun, 1989). That seasonal variations of flow velocity in Glacier No. 1 are not as large as in other large sub-polar glaciers in China is also evidence that little water reaches the bed, and that the extent of the unfrozen bed is limited.

4. GLACIER BED CHARACTERISTICS

It was found during excavation of the tunnels that there was an ice-laden till layer beneath the glacier. Electrical d.c. resistivity soundings conducted in the recently deglaciated area near the entrances of both tunnels in 1989 indicate that the till layer is 6.1 and 11.3 m thick in front of tunnels 1 and 2, respectively (Zeng and Qiu, 1991). Beneath the till layer the bedrock is also frozen. In addition, the glacier is surrounded by impermeable permafrost.

Based on the above descriptions, a schematic diagram (Fig. 3) was drawn to show the subglacial thermal, dynamic, and hydrological conditions for the east tributary. There is an ice-laden till layer beneath the glacier and upon the bedrock, which is > 10 m thick near the terminus and which is inferred to decrease in thickness gradually up-glacier. The 0°C isotherm is below the glacier sole, perhaps rising to the sole in the middle of the ablation area, and descends into bedrock through the ice-laden till layer near the terminus. Therefore the glacier is entirely cold and impermeable except for a thin snow–firn layer at its surface and some crevassed areas. Meltwater drains off mainly by surface channels, assisted by a few

https://doi.org/10.3189/1992AoG16-1-39-44 Published online by Cambridge University Press

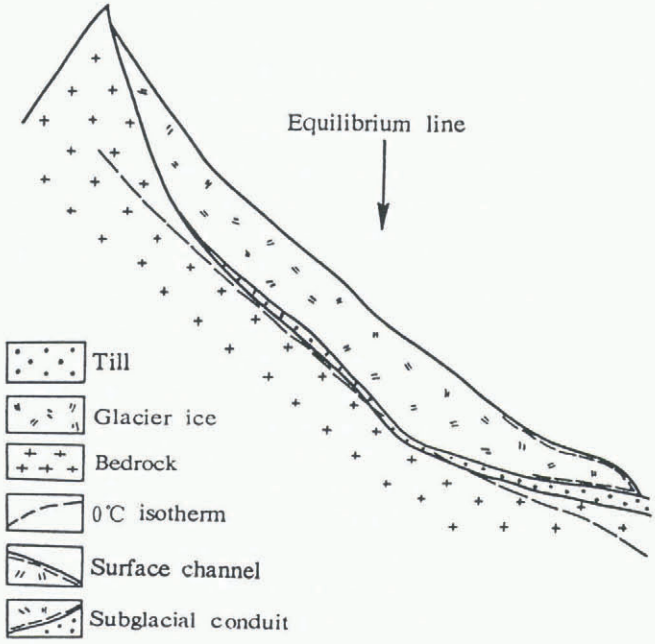

Fig. 3. Schematic diagram showing the subglacial thermal, dynamic and hydrological conditions.

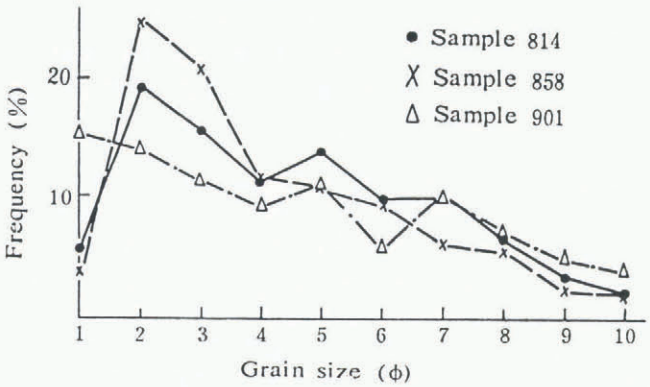

Fig. 4. Typical grain-size distributions for the debris in the ice-laden till. Only the grains smaller than 1 mm were analyzed.

subglacial conduits. Most of the water running through subglacial conduits comes from the glacier surface by way of marginal channels. It is possible that in the upper part of the ablation area the till layer between the glacier sole and the bedrock is unfrozen and saturated with water.

In this paper we regard the ice-laden till layer as a part of the glacier bed rather than a part of the basal ice because we believe that this layer has its own specific movement mechanism. In front of the glacier this layer is continuous with newly deglaciated deposits.

5. BED DEFORMATION

As shown in Figure 3, most of the glacier bed is believed to be a till-like layer, containing boulders, pebbles, sand and clay, of which a small portion in the middle ablation area is probably unfrozen and the rest is at sub-freezing temperatures. It is difficult to determine the mean ice content and size distribution of the debris because of its inhomogeneity. Some typical grain-size curves for the debris are shown in Figure 4. Only grains smaller than 1 mm were analyzed and plotted.

Direct observations in tunnel 1 have shown that most of the motion of the glacier is due to deformation of the ice-laden till bed at sub-freezing temperatures (Echelmeyer and Wang, 1987). The observations were made in a shaft, 34.7 m from the entrance, between 20 September and 11 November 1984. In order to reach the glacier bed, the shaft was excavated 3.5 m downward from the tunnel floor and bottomed ~0.35 m below the ice–till contact. Samples of the till at the base of the shaft contained 21–39% ice by weight. The solid material ranged in size from boulders to clay-size particles. The motion of a point just above the ice–till interface was approximately 8 mm d^{-1} relative to the base. This speed was approximately 60% of the surface speed, showing that a large part of the glacier movement at this point was due to deformation of the ice-laden till bed, which was ~0.35 m thick. The thickness of

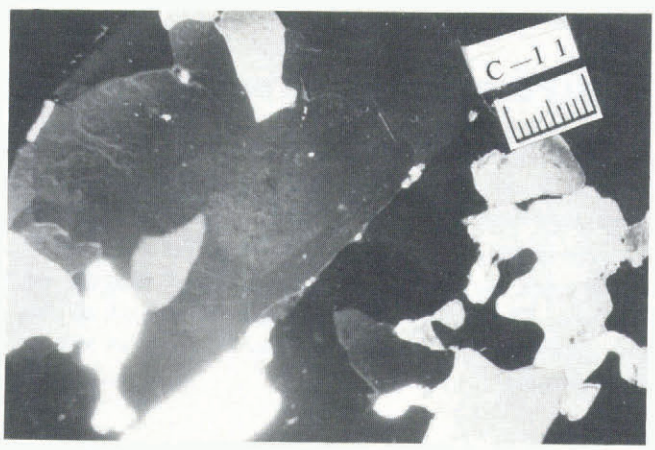

a

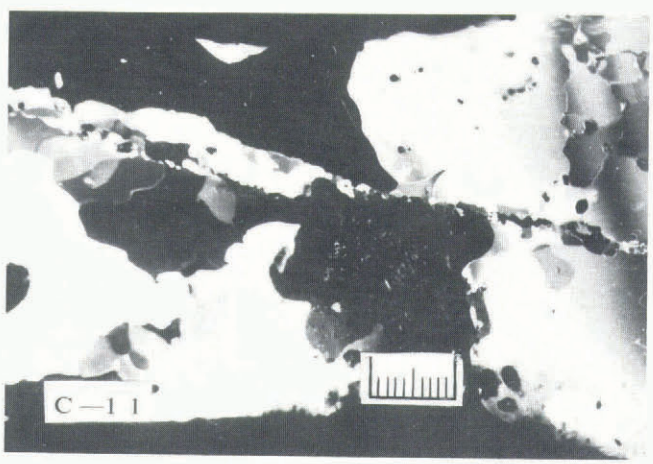

b

Fig. 5. Photographs of thin sections of ice under cross polaroids showing a possible shear plane (a) and a possible shear band (b) in the ice-laden till bed.

https://doi.org/10.3189/1992AoG16-1-39-44 Published online by Cambridge University Press

this layer was less than 2% of the total thickness of the glacier.

Echelmeyer and Wang (1987) treated the till as a thin boundary layer and compared the mean rate of shear strain across its 0.35 m thickness with that of the adjacent layer of ice. They assumed that the shear stress was approximately the same in the basal ice and the till, and thereby concluded that the mean effective viscosity for the ice is more than 100 times that of till.

On the other hand, a shear strain rate as large as $230 \times 10^{-4}\,d^{-1}$, as derived by Echelmeyer and Wang (1987), is quite high. It is possible that some slip along discrete shear planes occurs in the ice-laden till. Echelmeyer and Wang mentioned that macroscopic slip planes were not observed in the shaft mentioned above, but they did observe slip planes in the till at some other locations in tunnel 1, and substantial motion occurs across them.

Features that may be healed shear planes and shear bands in the debris-laden ice have been photographed (Fig. 5). Such features have been seen often. The photographed samples were taken from the till layer at the base of the glacier near where tunnel 1 used to be located. The photographs provide new evidence suggesting the occurrence of shear planes and shear bands within the till layer. Motion across such shear planes and shear bands would enhance the deformation of the till layer.

6. CREEP EXPERIMENTS ON DEBRIS-LADEN ICE

In 1989 samples were taken from the glacier bed near the location where tunnel 1 used to be. These were used for creep experiments under constant stress. By rejecting portions of the samples containing boulders and pebbles, debris-laden ice with a low debris concentration was obtained. The debris ranged in size from sand to clay. The grain-size distributions in Figure 4 are from some of these samples.

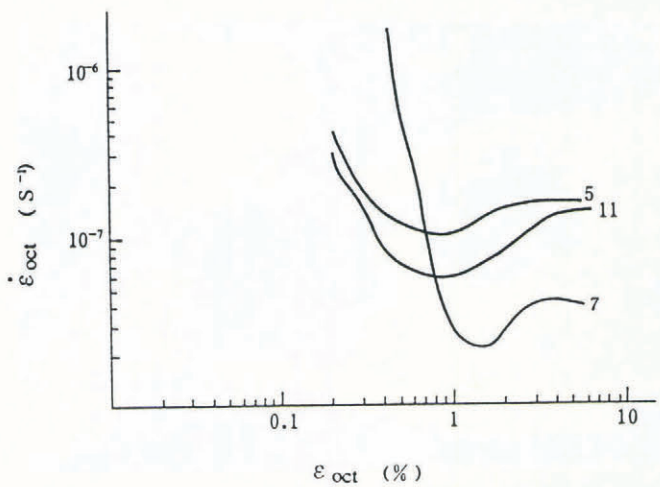

Fig. 6. Experimental relationship between octahedral shear strain rate and octahedral shear strain of glacier ice sample (11), and of debris-laden ice samples (5 and 7).

The samples were tested in two uniaxial creep testing machines. Each sample was machined to a cylinder, 200 mm in length and 113 mm in diameter, and then put into a plastic bag to avoid sublimation. The testing machine was able to keep a constant compressive stress, with an accuracy of ±1%. Experiments were carried out at a temperature of -1 ± 0.3°C and an octahedral stress of 0.2 MPa (or axial stress of 0.42 MPa). Two of the experimental results (5 and 7) are shown in Figure 6. The density, mean crystal diameter and debris concentration are $0.933\,g\,cm^{-3}$, 26.8 mm and 2.7% (by weight) for sample 5, and $0.945\,g\,cm^{-3}$, 29.4 mm and 7.1% (by weight) for sample 7. The tertiary octahedral strain rate, $\dot{\epsilon}_{oct}$, is 1.72 and $0.44 \times 10^{-7}\,s^{-1}$ for samples 5 and 7, respectively. Another result (11) plotted in Figure 6 is for clean ice. The density, mean crystal diameter and debris concentration of this sample were $0.868\,g\,cm^{-3}$, 18 mm and 0.03% (by weight), respectively. Before testing, all samples had multiple maxima *c*-axis fabrics, with several maxima situated around the original, in situ, vertical axis. The original vertical axis was set 45° to the compressive stress in the test. We can see from Figure 6 that as the loading starts, there is a work hardening for several tens of hours, ending with a minimum octahedral shear strain rate of $0.566 \times 10^{-7}\,s^{-1}$ when octahedral shear strain reached 1% or so. The deformation then changed gradually to a tertiary creep stage with a tertiary octahedral shear strain rate of $1.4 \times 10^{-7}\,s^{-1}$.

Usually a power law is used to describe the relation between effective strain rate, $\dot{\epsilon}$, and effective stress, τ:

$$\dot{\epsilon} = A\tau^n.$$

If, as usual, the exponent $n = 3$ is used, $A = 14.76$, 3.77 and $12.03 \times 10^{-15}\,kPa^{-3}\,s^{-1}$ for the tertiary creep stage and $A = 7.90$, 1.70 and $4.86 \times 10^{-15}\,kPa^{-3}\,s^{-1}$ for the minimum creep stage for experiments 5, 7 and 11, respectively.

Comparing the curves in Figure 6, we cannot see positive evidence for an increase in strain rate with increasing debris concentration in the samples. That is to say, the creep experiments failed to provide any positive information indicating that debris-laden ice deforms more easily than clean ice.

In 1990, experiments were carried out under the same conditions on laboratory-prepared polycrystalline ice mixed with carborundum powder of silt size. Five samples were tested, one of which was clean. The others contained respectively 9.8, 2.8, 10.6 and 11.4% carborundum powder by volume, or 30, 10, 31 and 33.4% by weight. These tests showed that adding silt enables ice to increase its strain rate by a factor of up to 3, which is far less than the factor of 100 suggested by Echelmeyer and Wang (1987). The experimental results are shown in Figure 7. The grain-size distribution of the carborundum powder was 24.2, 54.3 and 18.0% in the 4, 5 and 6ϕ size ranges, respectively. That is, 96.5% of the mixed powder is distributed between 4 and 6ϕ, the size of coarse silt. In contrast, the grain-size distribution of the ice-laden till had a larger percentage of coarse debris ($\phi < 4$) (cf. Figure 4 and Echelmeyer and Wang, 1987, fig. 3). Ice-crystal size in the laboratory-prepared samples was less than 5 mm and the *c* axes were randomly orientated.

Such an increase in strain rate has not been seen

https://doi.org/10.3189/1992AoG16-1-39-44 Published online by Cambridge University Press

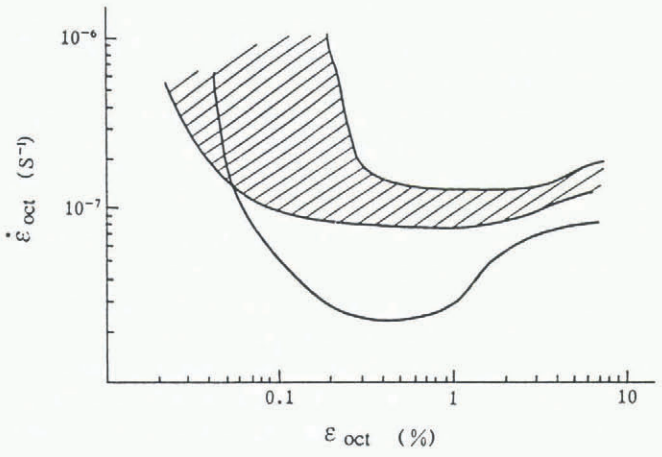

Fig. 7. Experimental relationship between octahedral shear strain rate and octahedral shear strain of laboratory-prepared dirty ice (shaded area) and clean ice (solid curve).

clearly in previous experiments (Hooke and others, 1972; Gao, 1989). There are two major differences. One is the grain-size of the debris, which was silt-sized in our experiments and sand-sized in the earlier experiments. Another is the test temperature. Our tests were carried out at −1°C which is higher than in the previous experiments. The influence of mixing fine debris on ice creep at high temperature seems significant.

In conclusion, it appears that the large mean shear strain rate of the debris-laden ice in situ found by Echelmeyer and Wang (1987) must be explained by discontinuous slip as mentioned in section 5.

7. SHEAR FAULTING AND SLIDING OVER THE BED

Early in the 1960s, Huang and others (1965) discovered that bands of fragmented crystals and shear planes appeared in basal ice exposed in a marginal channel. These bands showed high englacial shear. Four tracings were presented.

In the tunnels the flow is generally compressive. The dip of planes of maximum shear strain, which slope upward towards the tunnel entrance, decreases gradually from the back wall towards the entrance. Owing to the impediment of moraine deposits in front of the terminus, flow velocity decreases rapidly towards the terminus (Jing and others, 1992), and shear faulting, in which actively moving ice shears over more stagnant ice in front of it, could possibly be taking place along the direction of maximum shear strain.

It is thus believed that displacement along discrete shear zones may be one of the movement mechanisms of Glacier No. 1, although its contribution is small.

There is no direct observation of basal sliding over bedrock. However, in both tunnels, cavities were often seen down-flow from boulders embedded in the ice-laden till layer. The ice moving over the boulders was clean. Echelmeyer and Wang (1987) have measured a sliding rate of 0.5 mm d^{-1} over a solid rock surface in tunnel 1 under a shear stress of approximately 60 kPa. In addition, they have also observed discontinuous motion across interfaces between clean ice and underlying ice-laden till in some sections of tunnel 1.

8. CONCLUSION

Ürümqi Glacier No. 1 is a small cold glacier, lying on a till bed, most of which is frozen, ice-laden, and impermeable. The englacial and subglacial water conduits are not braided.

Four movement mechanisms have been identified. They are ice deformation, bed deformation, shear faulting, and sliding over the bed. In the terminus and marginal regions, where the glacier is thin, bed deformation, consisting of creep and discontinuous slip, can contribute significantly to the overall surface motion. Creep in the ice-laden bed is, in some cases, faster than in clean ice. Slip of discrete shear zones in the bed is probably the principal mechanism of bed deformation. Some of these shear zones may be, like those in Figure 5, in ice lenses in the till. Others may be in layers of till in which, perhaps due to the warm temperatures and the presence of solutes, there is some liquid water.

ACKNOWLEDGEMENTS

This research was supported by grants from the National Natural Science Foundation of China. The author is grateful to Wang Wenti, Ren Jiawen, Jin Zhengmei and Wang Xiaoxiang for their help in preparation of this paper.

REFERENCES

Cai Baolin. 1989. The research on the temperature in deep boreholes and temperature distribution modelling in Glacier No. 1, Ürümqi River headwaters. (Ph.D. thesis, Chinese Academy of Sciences. Lanzhou Institute of Glaciology and Geocryology. [In Chinese with English abstract.]

Cai Baolin, Huang Maohuan and Xie Zichu. 1988. A preliminary research on the temperature in deep boreholes of Glacier No. 1, Ürümqi headwaters. *Kexue Tongbao (Science Bulletin)*, **33**(24), 2054–2056.

Chen Yaowu and Sun Zuozhe. 1989. Surface movement velocity of Glacier No. 1 at the source of Ürümqi River during 1988–1989. *Annual Report on the Work at Tien Shan Glaciological Station*, 8, 97–103. [In Chinese.]

Echelmeyer, K. and Wang Zhongxiang. 1987. Direct observation of basal sliding and deformation of basal drift at sub-freezing temperatures. *J. Glaciol*, **33**(113), 83–98.

Gao Xiang Qun. 1989. Laboratory studies of the development of anisotropic crystal structure and the flow properties of ice. (Ph.D. thesis, University of Melbourne. Meteorology Department.)

Hooke, R. LeB, B. B. Dahlin and M. T. Kauper. 1972.

https://doi.org/10.3189/1992AoG16-1-39-44 Published online by Cambridge University Press

Creep of ice containing dispersed fine sand. *J. Glaciol.*, **11**(63), 327–336.

Hooke, R. LeB., J. E. Gould and J. Brzozowski. 1983. Near-surface temperatures near and below the equilibrium line on polar and subpolar glaciers. *Z. Gletscherkd. Glazialgeol.*, **19**(1), 1–25.

Huang Maohuan. 1990. On the temperature distribution of glaciers in China. *J. Glaciol*, **36**(123), 210–216.

Huang Maohuan and Wang Zhongxiang. 1987. Research on the tunnel excavated in Urumqi Glacier No. 1, Tianshan Glaciological Station, China. *J. Glaciol.*, **33**(113), 99–104.

Huang Maohuan, Xie Zichu and Mi Aili. 1965. A preliminary study of ice structure in Glacier No. 1, headwaters of Ürümqi River, Tien Shan mts. *In* Chinese Academy of Sciences. Institute of Geography. Division of Glaciology and Geocryology, *ed. Studies of glaciology and hydrology in Ürümqi River, Tien Shan mountains*. Beijing, Science Press, 31–37. [In Chinese.]

Huang Maohuan, Wang Zhongxiang, Cai Baolin and Han Jiankang. 1989. Some dynamics studies on the Urumqi Glacier No. 1, Tianshan Glaciological Station, China. *Ann. Glaciol.*, **12**, 70–73.

Huang Maohuan, Cai Baolin and Wang Zhongxiang. 1990. The basal conditions of the Glacier No. 1, Ürümqi River headwaters. *In Proceedings of the Fourth National Conference on Glaciology and Geocryology (Glaciology)*. Beijing, Science Press, 59–64. [In Chinese with English abstract.]

Jing Xiaoping, Huang Maohuan, Chen Jianming and Jin Mingxie. 1992. Basal deformation of Ürümqi Glacier No. 1, Tien Shan mountains, China. *Ann. Glaciol.*, **16**, 123–126.

Kang Ersi. 1991. A preliminary study on the drainage system in the ablation area of the Glacier No. 1 at the source of Ürümqi River. *J. Glaciol. Geocryol.*, **13**(3), 217–228. [In Chinese with English abstract.]

You Genxiang. 1987. Surface movement velocity of Glacier No. 1 at the head of Ürümqi River. *Annual Report on the Work at Tien Shan Glaciological Station*, 4, 81–87. [In Chinese.]

Zeng Zhonggong and Qiu Guoqing. 1991. Explanation of electrical D.C. resistivity sounding at the head waters of Ürümqi River, Tien Shan. *J. Glaciol. Geocryol.*, **13**(2), 176–179. [In Chinese with English abstract.]

Zhang Xiangsong, Zhu Guocai, Qian Songlin, Chen Jiyang and Shen Ying. 1985. Radar measuring ice thickness of No. 1 Glacier at the source of Ürümqi River, Tien Shan. *J. Glaciol. Geocryol.*, **7**(2), 153–162. [In Chinese with English abstract.]

The accuracy of references in the text and in this list is the responsibility of the author/s, to whom queries should be addressed.

https://doi.org/10.3189/1992AoG16-1-39-44 Published online by Cambridge University Press